

# Emissions of Intermediate- and Semi-Volatile Organic Compounds (I/SVOCs) from Different Cumulative Mileage Diesel Vehicles under Various Ambient Temperatures

Shuwen Guo<sup>1</sup>, Xuan Zheng<sup>1\*</sup>, Xiao He<sup>1</sup>, Lewei Zeng<sup>1</sup>, Liqiang He<sup>2</sup>, Xian Wu<sup>2</sup>, Yifei Dai<sup>3</sup>, Zihao Huang<sup>1</sup>,  
5 Ting Chen<sup>4</sup>, Shupeixiao<sup>1</sup>, Yan You<sup>5</sup>, Sheng Xiang<sup>6</sup>, Shaojun Zhang<sup>4</sup>, Jingkun Jiang<sup>4</sup>, and Ye Wu<sup>4</sup>

<sup>1</sup>College of Chemistry and Environmental Engineering, Shenzhen University, Shenzhen 518060, China

<sup>2</sup>State Environmental Protection Key Laboratory of Vehicle Emission Control and Simulation, Chinese Research Academy of Environmental Sciences, Beijing 100012, China

<sup>3</sup>Institute for Advanced Study, Shenzhen University, Shenzhen 518060, China

10 <sup>4</sup>School of Environment, State Key Joint Laboratory of Environment Simulation and Pollution Control, Tsinghua University, Beijing 100084, China

<sup>5</sup>National Observation and Research Station of Coastal Ecological Environments in Macao, Macao Environmental Research Institute, Macao University of Science and Technology, Macao SAR 999078, China

<sup>6</sup>State Key Laboratory of Pollution Control and Resource Reuse, Tongji University, Shanghai, China 200092, China

15 *Correspondence to:* Xuan Zheng (x-zheng11@szu.edu.cn)

**Abstract.** The role of intermediate- and semi-volatile organic compounds (I/SVOCs) in heavy-duty diesel vehicle (HDDV) exhaust remains a significant research gap across previous studies, with limited focus on cumulative mileage and ambient temperature effects. This study analyzed gaseous and particulate I/SVOCs from four in-use HDDVs using thermal desorption two-dimensional gas chromatography-mass spectrometry (TD-GC×GC-MS). Total I/SVOC emission factors (EFs) ranged  
20 from 9 to 406 mg·km<sup>-1</sup>, with 79 – 99 % in the gaseous phase. High-mileage vehicles (HMGVs) emitted I/SVOCs at levels eight times greater than low-mileage vehicles (LMVs), highlighting the influence of cumulative mileage. Emission deterioration occurred under both cold-start and hot-running conditions, though HMGVs showed no extra sensitivity to cold starts. HMGVs also exhibited increasing emissions with component volatility, alongside a higher proportion of oxygenated I/SVOCs (O-I/SVOC) than LMVs (65% vs. 42%). Unique compounds such as phenol, alkenes, and cycloalkanes were detected exclusively  
25 in HMGV emissions. Temperature effects were most pronounced at 0°C, where only HMGV emissions increased significantly, while LMV emissions remained relatively stable. A strong linear correlation ( $R^2 = 0.93$ ) between I/SVOC EFs and modified combustion efficiency (MCE) suggested that reduced combustion efficiency is a key driver of higher I/SVOC emissions. HMGVs also showed four times greater secondary organic aerosol formation potential (SOAFP) compared to LMVs. This increase was smaller than the eightfold rise in EFs, likely due to the higher O-I/SVOC content in HMGV emissions.

30

**Keywords.** HDDVs, I/SVOCs, emission deterioration, cumulative mileage, ambient temperature, combustion efficiency

## 1 Introduction

As a major air pollutant, fine particulate matter (PM<sub>2.5</sub>) leads to over three million premature deaths globally each year (Apte

et al., 2018), mainly associated with lung cancer, ischemic heart disease, and stroke (Guan et al., 2018; Xue et al., 2021).  
35 Secondary organic aerosol (SOA) accounts for 12% to 77% of the total PM<sub>2.5</sub> mass based on global source apportionment  
results (Huang et al., 2014; Sun et al., 2020; Zhang et al., 2021). Observation studies have demonstrated that SOA contributions  
increase with the severity of pollution during haze episodes in megacities in China (He et al., 2020; Ho, 2016; Li et al., 2015;  
Azmi et al., 2023; Wang et al., 2023; Wang et al., 2024). Among potential SOA precursors, intermediate-volatility and semi-  
volatile organic compounds (I/SVOCs), with effective saturation concentrations ( $C^*$ ) between  $10^3$  to  $10^6$  and  $10^0$  to  $10^2$   $\mu\text{g}\cdot\text{m}^{-3}$ ,  
40 <sup>3</sup>, have been demonstrated to be more effective than volatile organic compounds (VOCs) (Daniel S. Tkacik et al., 2012; Jathar  
et al., 2013; Morino et al., 2022; Presto et al., 2009; Sommers et al., 2022; Huang et al., 2023).

Heavy-duty diesel vehicles (HDDVs) are recognized as significant sources of I/SVOCs (Alam et al., 2018; Drozd et al., 2021;  
Liu et al., 2021; Lu et al., 2018; Presto et al., 2009; Zhao et al., 2015). However, the contribution of HDDVs to I/SVOC  
emissions from on-road motor vehicles in China remains a contentious topic as indicated by different studies. For example,  
45 Zhao et al. (2022) reported that diesel vehicles contributed 85% of IVOC emissions from on-road mobile sources in China,  
while Chang et al. (2022) found that diesel vehicles emitted only about 20% of the IVOCs produced by gasoline vehicles.  
These discrepancies highlight the urgent need for a more precise assessment of diesel vehicle I/SVOC emission factors (EFs).  
Previous studies have explored the impact of emission standards, after-treatment technologies, and driving cycles on EFs (Zhao  
et al., 2015; He et al., 2022b, a; Zhang et al., 2024a), while the influence of cumulative mileage and low ambient temperatures  
50 on HDDV emissions remains unexplored. Given that many regions in China experience temperatures below 0°C during winter,  
evaluating how HDDVs operate under such conditions is critical in I/SVOC emissions and exhaust component distribution  
across different temperature conditions.

The complexity of I/SVOC components poses a challenge in accurately measuring HDDV EFs. The alkanes, alkenes, alkynes,  
cycloalkanes, monocyclic aromatic compounds, and oxygenated organic compounds present in IVOCs are all significant  
55 precursors of SOA. Previous analyses of I/SVOCs primarily relied on traditional one-dimensional gas chromatography coupled  
with mass spectrometry (GC-MS). Due to limitations in separation techniques, many challenging-to-analyze I/SVOCs are  
grouped as an unresolved complex mixture (UCM), allowing for only rough quantification (Liu et al., 2021; Qi et al., 2019,  
2021; Tang et al., 2021; Zhao et al., 2014, 2015, 2016). For example, Zhao et al (2015) reported that 80% of I/SVOCs emitted  
by diesel vehicles were classified as UCM. This lack of detailed chemical information introduces uncertainties in I/SVOC  
60 quantification and prediction of SOA formation potential (SOAFP) (He et al., 2022b).

To address these challenges, our previous studies (He et al., 2022a, b) employed comprehensive two-dimensional gas  
chromatography (GC×GC), which enhances selectivity, peak capacity, and sensitivity by connecting two capillary columns  
with complementary stationary phases in series. We developed a method by constructing class-screening programs based on  
characteristic fragments and mass spectrum patterns to identify thousands of organic compounds using GC×GC, which  
65 successfully identified over 85% of I/SVOCs from HDDV exhaust (He et al., 2022b). Furthermore, we also quantify  
oxygenated I/SVOCs (O-I/SVOCs) and find the identified O-I/SVOCs result in a 45% difference in the prediction results of  
SOAFP (He et al., 2022b). Therefore, the application of GC×GC and the qualitative method based on the unique mass spectrum  
patterns for I/SVOC (He et al., 2022a, b, 2024), provides a more accurate determination of I/SVOC EFs and component  
distribution. This methodology offers a robust foundation for analyzing the effects of cumulative mileage and ambient  
70 temperatures on HDDV I/SVOC emissions.

In this study, a thermal desorption two-dimensional gas chromatography and mass spectrometry (TD-GC×GC-MS) was  
utilized to analyze gaseous and particulate I/SVOCs emitted from four HDDVs in chassis dynamometer tests. The I/SVOC  
EFs, gas-to-particle partitioning, and detailed chemical species across vehicles with different cumulative mileages under

75 different ambient temperatures were reported. The role of combustion efficiency in influencing I/SVOC emissions was explored. Additionally, the SOAFP of I/SVOCs in the exhaust of different vehicles was evaluated. The impact of cumulative mileage and ambient temperature on total I/SVOC emissions in the emission inventory was assessed after incorporating these factors into the EFs.

## 2 Materials and methods

### 2.1 Fleet and dynamometer tests

80 Four in-use HDDVs using China VI 0# diesel fuel were tested on a chassis dynamometer following China heavy-duty commercial vehicle test cycle for tractor trailers (CHTC-TT) at the China Automotive Technology & Research Center (CATARC) in Guangzhou, China. All tested HDDVs were equipped with selective catalytic reduction (SCR) systems and complied with the China V national emission standard. Two vehicles with lower cumulative mileage were numbered as D1 and D2 (low-cumulative mileage vehicles, LMVs), while the other two with higher cumulative mileage were labeled as D3 and D4 (high-cumulative mileage vehicles, HMsVs). To assess the impact of ambient temperature on I/SVOC emissions, emission tests for D2 and D4 were conducted both at 0°C and 23°C. General information about the vehicles is presented in Table 1. The sets of test cycles are listed in Table S1.

**Table 1. Information on the test fleet**

| Vehicle ID  | D1        | D2         | D3          | D4          |
|---|-----------|------------|-------------|-------------|
| <b>Emission Standard</b>                                | China V   | China V    | China V     | China V     |
| <b>Aftertreatment Devices</b>                           | SCR       | SCR        | SCR         | SCR         |
| <b>Brand</b>  | DONGFENG  | SINOTRUK   | DELONG      | DELONG      |
| <b>Engine Model</b>                                     | dCi450-51 | MC13.54-50 | WP10.310E53 | WP10.310E53 |
| <b>Used Duration</b>                                    | 7 months  | 8 months   | 32 months   | 32 months   |
| <b>Cumulative Mileage</b><br>( $\times 10^3$ km)        | 22.21     | 34.84      | 169.50      | 188.33      |
| <b>Gross Combined Weight</b><br><b>Rating (GCWR, t)</b> | 48.8      | 48.8       | 41.8        | 41.8        |
| <b>Rated Power</b><br><b>(kW)</b>                       | 309       | 397        | 228         | 228         |
| <b>Displacement (L)</b>                                 | 11.12     | 12.42      | 9.73        | 9.73        |

Each CHTC-TT lasts 1800 seconds, with an average speed of  $46.6 \text{ km}\cdot\text{h}^{-1}$  and a maximum speed of  $88 \text{ km}\cdot\text{h}^{-1}$  (Fig. S1).  
90 When the vehicles were driven at the speed specified by the CHTC-TT on the dynamometer, the emitted exhaust from tailpipes was diluted in the constant volume sampler (CVS). The exhaust dilution ratio was about 40. The CVS system maintains the airflow of the diluted exhausts at 25°C to avoid thermophoretic and condensational losses. CO<sub>2</sub>, CO, total hydrocarbons (THC), and NO<sub>x</sub> from the diluted exhaust were detected by the real-time gas analyzer module (MEXA-7400HLE, HORIBA, Japan) provided by the CATARC, and a series of offline sampling test samples were also collected from the CVS.

### 95 2.2 Sampling and analysis

The diluted exhaust from CVS was filtered with a 47 mm PTFE filter (R2PJ047, PALL Corporation, USA) and then collected

by the Tenax TA tubes (C1-AAXX-5003, MARKES International, UK) and 47mm quartz filters (Grade QM-A, Whatman, UK), respectively, for analyzing I/SVOCs and gas-phase organic compounds adsorbed on quartz filters ( $Q_{\text{gas}}$ , Fig. S2.). Note that 2 TA tubes were connected in series for each sampling to prevent penetration, and the quantitative results of the two connected tubes were ultimately added together. Particulate matters in the exhaust from CVS were also captured by another parallel pipe with a 47mm quartz filter ( $Q_{\text{total}}$ ) for analyzing the particulate organic compounds, mainly including I/SVOCs. The accurate mass of particulate organics was obtained by subtracting  $Q_{\text{gas}}$  from  $Q_{\text{total}}$  to avoid adsorption of gaseous organic compounds.  $Q_{\text{gas}}$  accounted for 32% of  $Q_{\text{total}}$  as detailed in Sect. 3.2. Thus, the total I/SVOC results in this paper were gaseous I/SVOCs collected by TA tubes plus particulate I/SVOCs collected by quartz filters after deducting artifacts (total I/SVOCs =  $TA + (1 - 32\%) \times Q_{\text{total}}$ ). Notably, the gas phase of I/SVOCs was collected after passing through a PTFE filter, but the separation of gas and particle I/SVOCs beyond the PTFE filter may disrupt the equilibrium between them. This disruption could cause the evaporation of particle I/SVOCs, potentially leading to an overestimation of  $Q_{\text{gas}}$  (Cheng et al., 2010). Cheng et al. (2010) evaluated the collection artifacts of organic carbon using various quartz filter sampling methods and found that about 10% of the  $Q_{\text{gas}}$  derived from volatilized particulate organic carbon by the sampling method used in this study. Therefore, the  $Q_{\text{gas}}$  in this study may be slightly overestimated. The TA tubes were prebaked at 320°C for 2 hours and at 335°C for 30 minutes. The quartz filters were also prebaked for 8 hours at 550°C in a muffle furnace to remove carbonaceous contamination. All quartz filter samples were stored at -20°C.

Each TA tube was injected with 2  $\mu\text{L}$  of deuterated internal standard mixing solution (IS) through a mild nitrogen blow (CSLR, MARKES International, UK) before TD-GC $\times$ GC-MS analysis. The TD-GC $\times$ GC-MS system was composed of an autosampler with a thermal desorber (ULTRA-xr<sup>TM</sup> and UNITY-xr<sup>TM</sup>, MARKES International, UK) and a solid-state modulator (SSM1810, J&X Technologies, China) installed on a gas chromatograph (8890, Agilent Technologies, USA) coupled with a mass spectrometer (5977 B, Agilent Technologies, USA). The quartz filter samples were also injected with the same IS and then inserted into clean quartz tubes (C0-FXXX-0000, MARKES International, UK) for TD-GC $\times$ GC-MS analysis.

In the thermal desorption unit, TA tube (quartz filter) samples were heated at 320°C (330°C) for 20 min with a trap flow of 50  $\text{mL}\cdot\text{min}^{-1}$ , and then all desorbed organics were captured by the cold trap (U-T1HBL-2S, MARKES International, UK). Subsequently, the cold trap was heated at 330°C (340°C) for 5 min so that the organics could enter GC $\times$ GC to be separated and detected by MS. In GC $\times$ GC, 4 different columns (Agilent Technologies, USA) were connected in series, from front to back: 30 m DB-5MS, 0.6 m VF-1ms, 0.7 m CP802510 (open tubular column), and 1.2 m DB-17MS. Among them, VF-1ms switched between the cold and hot zones of the modulator. Hence, the organics that undergone the first separation entered the subsequent columns in the form of a pulse for the second separation. The oven of 8890 and hot zone of the modulator matched the same heating program: maintained at 50°C for 3 min, then increased to 310°C at a rate of 5°C $\cdot\text{min}^{-1}$  and maintained for 5 min. The cold zone of the modulator dropped from 9°C to -51°C at the fastest speed and maintained for 21.8 min, and then rose to 9°C at a rate of 20°C $\cdot\text{min}^{-1}$  and maintained for 34 min.

### 2.3 Qualitative analysis and quantification of I/SVOCs

The I/SVOCs were identified and quantified with their respective authentic standards or surrogates using the three-step approach proposed by He et al. (2022b). Given that more than fifteen hundred peaks were typically observed, it was not feasible to accurately identify and quantify every individual peak. To address this, the organic compounds in the samples were categorized into eleven groups, each associated with a specific mass spectrometry rule under electron energy 70 eV. The peaks without external standard curves (ES) were quantified by the closest and same group ES. A total of 120 ES were used in this study to cover as many organic compounds as possible, as shown in Fig. S3. All group identification codes and information on ES are listed in Table S2. The elution peak area that cannot be recognized by any identification code accounts for about 20%

of the total peak area, which was not quantified in this study.

## 2.4 Emission factor calculation

All pollutant data were reported as distance-based and fuel-based emission factors (EFs):

$$140 \quad EF_{d,i} = \frac{\Delta m_i}{s} \quad (1)$$

$$EF_{f,i} = \frac{\Delta m_i w_C}{12/44 \cdot \Delta CO_2 + 12/28 \cdot \Delta CO} \quad (2)$$

where  $\Delta m_i$  is the measured background-corrected mass of species  $i$  (mg).  $s$  is the distance traveled by the vehicle in a test cycle (km).  $w_C$  is the measured carbon mass fraction of fuel, of 0.82.  $\Delta CO_2$ ,  $\Delta CO$  and are the background-corrected masses of  $CO_2$  and  $CO$ .

## 145 2.5 Modified combustion efficiency (MCE) calculation

MCE was applied herein to represent the combustion efficiency in each measurement, as displayed in:

$$MCE = \frac{\sum_{i=1}^n \frac{[CO_2]_i}{[CO_2]_i + [CO]_i}}{n} \quad (3)$$

where  $[CO_2]_i$  and  $[CO]_i$  are instantaneous mixing ratios of  $CO_2$  and  $CO$  at second  $i$ , respectively, during the entire cycle where  $n$  is equal to 1800 s.

## 150 2.6 Emission Inventory Calculation

According to the official guide (Ministry of Ecology and Environment of the People's Republic of China, 2024) and the national HDDV population in 2022, the emission inventory was established based on:

$$E_n = \sum P \times VKT \times EF_n \quad (4)$$

155 where  $E_n$  is the total mass of I/SVOC emissions of different cases in this study.  $P$  is the vehicle population.  $VKT$  represents the calibrated annual kilometers traveled per vehicle, which is considered 87786.15 km ( $240.51 \text{ km} \cdot \text{d}^{-1} \times 365 \text{ d}$ ) for each freight vehicle (Anon, 2022).  $EF_n$  is emission factor of I/SVOCs of different cases in  $\text{mg} \cdot \text{km}^{-1}$ . 3 cases are assumed in this study.

## 2.7 SOAFP estimation

160 The SOAFP derived from I/SVOCs was estimated followed the approach of Zhao et al (Zhao et al., 2015), and the detailed parameterizations were listed in SI. The SOAFP ( $\text{mg} \cdot \text{km}^{-1}$ ) produced over a period ( $\Delta t$ ) was calculated as follows:

$$SOAFP = \sum [EF_i \times (1 - \exp(-K_{OH_i} \times [OH] \times \Delta t)) \times Y_i] \quad (5)$$

where  $EF_i$  is emission factor of pollution  $i$  in  $\text{mg} \cdot \text{km}^{-1}$ .  $K_{OH_i}$  is the hydroxyl (OH) radical reaction rate constant of compound  $i$  at  $25^\circ\text{C}$ .  $[OH]$  is the OH concentration, assumed to be  $1.5 \times 10^6 \text{ molecules} \cdot \text{cm}^{-3}$ .  $\Delta t$  is the photooxidation time (s).  $Y_i$  is the SOA yield of precursors  $i$ .

## 165 3. Results and discussion

### 3.1 Overall results

170 The HDDV I/SVOC EFs ranged from 9 to  $406 \text{ mg} \cdot \text{km}^{-1}$  ( $41$  to  $1848 \text{ mg} \cdot \text{kg-fuel}^{-1}$ ) in this study, consistent with previous findings, indicating a broad range of I/SVOC EFs from HDDVs. For example, Zhao et al. (2015) reported that the IVOC EFs of assorted heavy-duty vehicles were 17 to  $5354 \text{ mg} \cdot \text{kg-fuel}^{-1}$ , with various driving cycles and after-treatments. Similarly, He et al. (2022b) manifested that the I/SVOC EFs of China IV and China VI HDDVs ranged from 38 to  $18900 \text{ mg} \cdot \text{kg-fuel}^{-1}$ , attributing this extensive range to the significant differences in after-treatments and emission standards of vehicles. Zhang et al. (2024a) tested two China V HDDVs and reported that the gaseous I/SVOC EFs were 2034 and  $2054 \text{ mg} \cdot \text{kg-fuel}^{-1}$ ,

respectively.

To further analyze the I/SVOCs component and volatility distribution, the average EFs of all test cycles were divided into seven intervals based on  $\log_{10}C^*$ , as shown in Fig. S4. Overall, IVOCs dominated the I/SVOC emissions with an average contribution of 81%, with the remaining 19% attributed to SVOCs. The primary contributors to the total identified EFs, ranked from high to low, were alkanes (including *n*- and *i*-alkanes, 20%), oxy-PAH & oxy-benzene (20%), phenol (14%), acid (11%), PAH\_3rings (11%), alcohol (10%), and carbonyls (7%). The proportion of O-I/SVOC (including alcohols, phenols, carbonyls, acids, oxy-PAHs, and oxy-benzenes) accounted for 61% of the total. The proportions of other categories were lower than 5%.  
The proportion of O-I/SVOCs was notably higher in this study compared to previous research, where alkanes typically accounted for 37% to 66% and O-I/SVOCs for 20% to 27% (He et al., 2022b; Zhang et al., 2024a). The discrepancy may relate to differences in the types of vehicles tested and variations in the composition of diesel and lubricating oils. Most of the detected alkanes in this study were present in relatively higher-volatility bins like bin 6 ( $\log_{10}C^* = 6$ ), while PAHs were distributed across bin 1 to 4. For O-I/SVOCs, alcohols and phenols mainly fell into bin 5, while oxy-PAHs & oxy-benzenes exhibited decreasing concentrations with decreasing volatility. Although a higher acid proportion was detected in this study compared to previous work (He et al., 2022b; Zhang et al., 2024a), their contribution to SOA production was considered minimal due to their low SOA yields (Huang et al., 2024).

### 3.2 Gas-particle partition and I/SVOC artifacts on quartz filters

Generally, the gaseous I/SVOCs consistently accounted for 79% to 99% of the total I/SVOCs, while particulate I/SVOCs contributed 1% to 21%. However, Liu et al. (2021) reported that China V HDDVs could emit more particulate I/SVOCs than gaseous I/SVOCs. This discrepancy may be attributed to the use of series sampling with a quartz filter and a TA tube, which can lead to the adsorption of a substantial fraction of gaseous I/SVOCs onto the quartz filters (artifacts), causing these compounds to be mistakenly categorized as particulate-phase. At the same time, the adsorption on the front quartz filters reduces the amount of gaseous I/SVOCs that reach the rear TA tubes, resulting in the final calculated proportion of particulate I/SVOCs exceeding 50%.

To assess the impact of adsorption artifacts on quartz filters,  $Q_{\text{gas}}$  samples from the hot-start cycles of the tested vehicles were analyzed. Results indicated that artifacts accounted for  $32\% \pm 14\%$  of the mass fractions on quartz filters, consistent with previous findings (May et al. 2013). Including these artifacts directly in the particulate-phase measurement introduces significant uncertainty into the calculated emission inventory, especially for IVOCs, and amplifies the uncertainties in environmental impact predictions related to emission sources. As illustrated in Fig. S5(a), IVOCs dominated the artifacts on quartz filters, representing 98% of the mass, while SVOCs made up only 2%. From a chemical composition perspective, carbonyls were the most affected by adsorption artifacts (Fig. S5(b)). However, accurately determining the adsorption capacity of quartz filters for gaseous I/SVOCs or predicting the point of saturation remains a challenge due to variability in filter properties across different manufacturers and production batches (Kirchstetter et al. 2001). Therefore, it is essential to minimize or eliminate particle quantification errors caused by adsorption artifacts to reduce uncertainties in subsequent modeling efforts. This is particularly crucial when assessing the environmental impact of IVOCs, given their substantial role in SOA formation and pollution forecasting.

### 3.3 I/SVOC EFs and composition from HDDVs with varying cumulative mileage

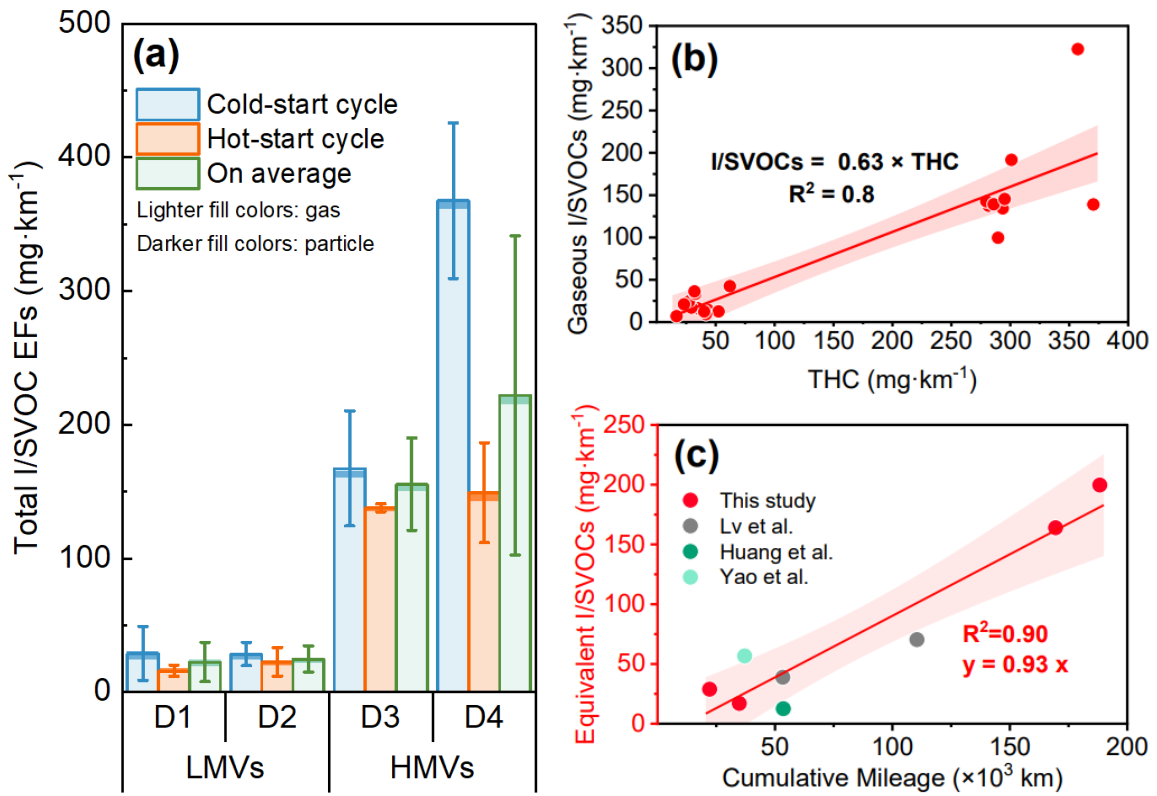
Figure 1(a) presents the distance-based EFs of I/SVOCs for HMTVs and LMTVs. The data reveal that the average I/SVOCs EFs of HMTVs (D3&D4,  $190 \pm 94 \text{ mg}\cdot\text{km}^{-1}$ ) were approximately eight times higher than those of LMTVs (D1&D2,  $23 \pm 11 \text{ mg}\cdot\text{km}^{-1}$ ), even HMTVs consumed less fuel on average ( $26 \text{ L}\cdot 100\text{km}^{-1}$ ) compared to LMTVs ( $33 \text{ L}\cdot 100\text{km}^{-1}$ ) for their lower GCWR. The significant disparity in I/SVOC EFs between HMTVs and LMTVs indicates that cumulative mileage is a critical

factor influencing I/SVOC EFs ( $p = 0.005$  for hot-start cycles), which has often been overlooked in previous studies. For instance, both the official guideline (Ministry of Ecology and Environment of the People's Republic of China, 2024) and the COPERT 4 model, the latest vehicular emission factor model (Cai and Xie, 2013), do not account for the deterioration of organic emissions (e.g., THC) from diesel vehicles.

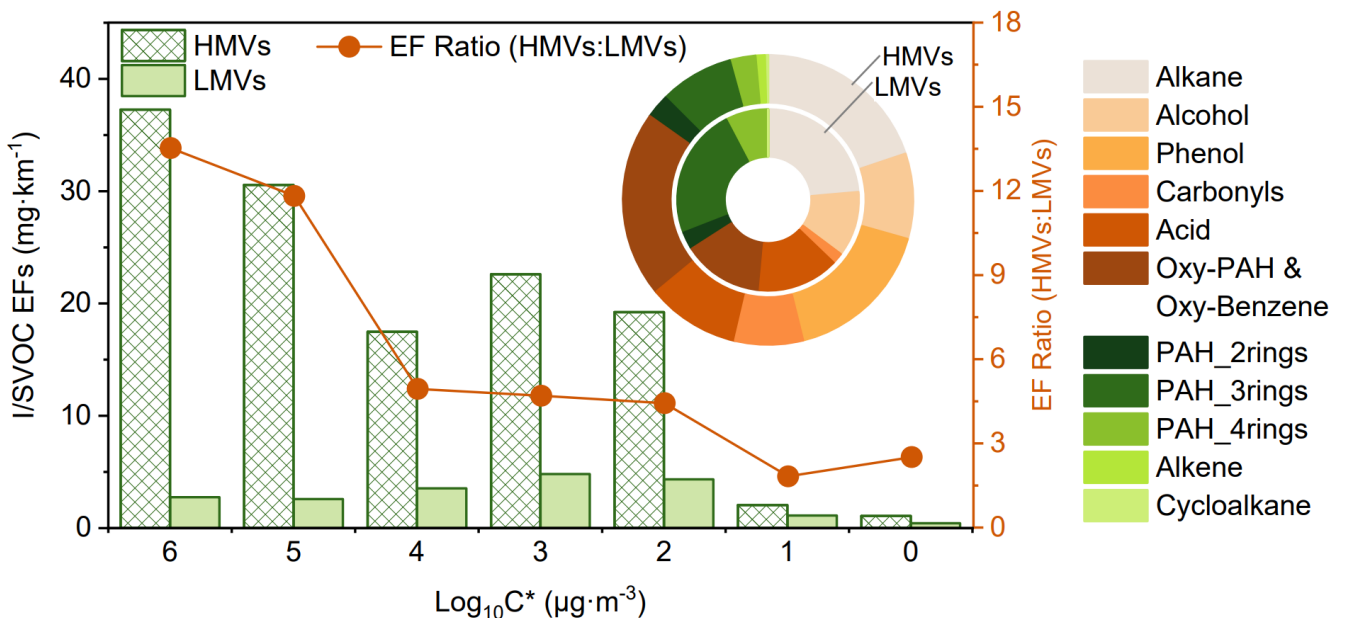
To investigate the underlying causes of high I/SVOC emissions from HMVs, we compared the MCE of each test cycle. As shown in Fig. S6, a strong correlation ( $R^2 = 0.73$ ) was observed between MCE and I/SVOC EFs. As combustion efficiency decreases, I/SVOC EFs rise, and HMVs exhibit greater variability in MCE than LMVs. This suggests that cumulative mileage contributes to increased emissions, emphasizing the need to incorporate this factor into emission inventories and SOA estimation. Given the scarcity of I/SVOC EF data in previous studies (Huang et al. 2013, Yao et al. 2015, Lv et al. 2020), we estimated the emission deterioration factors of I/SVOCs by leveraging the strong correlation between THC and I/SVOC emissions and available THC EFs. Figure 1(c) demonstrates a linear relationship ( $R^2 = 0.9$ ) between equivalent I/SVOCs and cumulative mileage. It should be noted that existing research primarily focuses on diesel vehicles with cumulative mileage below 200,000 km. Further experiments are necessary to determine whether I/SVOC emissions from designated HDDVs with over 200,000 km of mileage continue to increase linearly or stabilize. Also, the brand, engine models, GCWR, and displacement of the four HDDVs were slightly different (Table 1), which might bring some uncertainty to the emission analysis results (Zeng et al., 2024; Tolouei and Titheridge, 2009; Aosaf et al., 2022). Future studies should further consider the uncertainties brought by these factors.

Additionally, we examined the cold-start extra emissions (CSEE), which is the difference between emissions from the cold-start cycle and hot-start cycle results. For HMVs, CSEE ranged from 657 to 5592 mg, whereas for LMVs, it ranged from 79 to 281 mg. CSEE contributed 18% to 59% of the total cold-start cycle emissions for HMVs and 21% to 45% for LMVs, respectively. It indicated that the I/SVOC emission deterioration could occur under both the cold-start and hot-running conditions.

To further compare volatility and category distribution, the average EFs of HMVs and LMVs are shown separately in Figure 2. The EF ratios across different volatility bins exhibited a decreasing trend with decreasing volatility, indicating that the elevated I/SVOC EFs of HMVs were primarily due to a marked increase in organics within the volatility range of bins 2 to 6. Figure 2 further depicts the relative proportion of distinct organic groups present in I/SVOC emissions and their EFs are shown in Fig. S8. The EFs of all organic compounds emitted by HMVs were higher than those of LMVs, but the magnitude of the increase varied. Except for phenol, alkene, and cycloalkane, the organic group with the highest HMV-LMV ratio was carbonyls, up to 34, as shown in Fig. S8. The next highest is oxy-PAH & oxy-benzene, whose HMV-LMV ratio reached 11. The ratios of PAH\_2rings, alcohol, and alkane were 7. Overall, the HMV-LMV ratios of O-I/SVOCs were relatively higher, which contributed 65% of the I/SVOCs emissions from HMVs, compared to 42% for LMVs. Since the SOA yields of O-I/SVOCs are lower than those of hydrocarbon-like I/SVOCs in the same bin (Chacon-Madrid and Donahue, 2011), variations in O-I/SVOC proportions directly impacted the SOAFP gap between HMVs and LMVs, which would be further discussed in Sect. 3.5. Alkane and oxy-PAH & oxy-benzene were the dominant contributors to I/SVOCs for both HMVs and LMVs. PAH\_3rings contributed 8% of the I/SVOC emissions for HMVs, but 23% for LMVs. Interestingly, phenol, alkene, and cycloalkane were not detected in any of the LMV samples.



250 **Figure 1. (a) The bar chart represents total I/SVOC EFs from each HDDV under cold- and hot-start driving cycles.**  
 The error bars are standard deviations. Gaseous and particulate I/SVOCs were represented by the lighter and darker fill  
 colors respectively. The horizon axis is vehicle ID. **(b) The linear correlation between gaseous I/SVOC and THC EFs. (c)**  
**The linear correlation between THC EFs and HDDV cumulative mileage.** Data are from this study and previous studies  
 (Huang et al., 2013; Lv et al., 2020; Yao et al., 2015), of which tested vehicles shared the same THC emission limit (China  
 255 IV/V and Euro IV/V emission standards limit diesel engines THC EF to 460 mg·kWh<sup>-1</sup>) and similar weight.



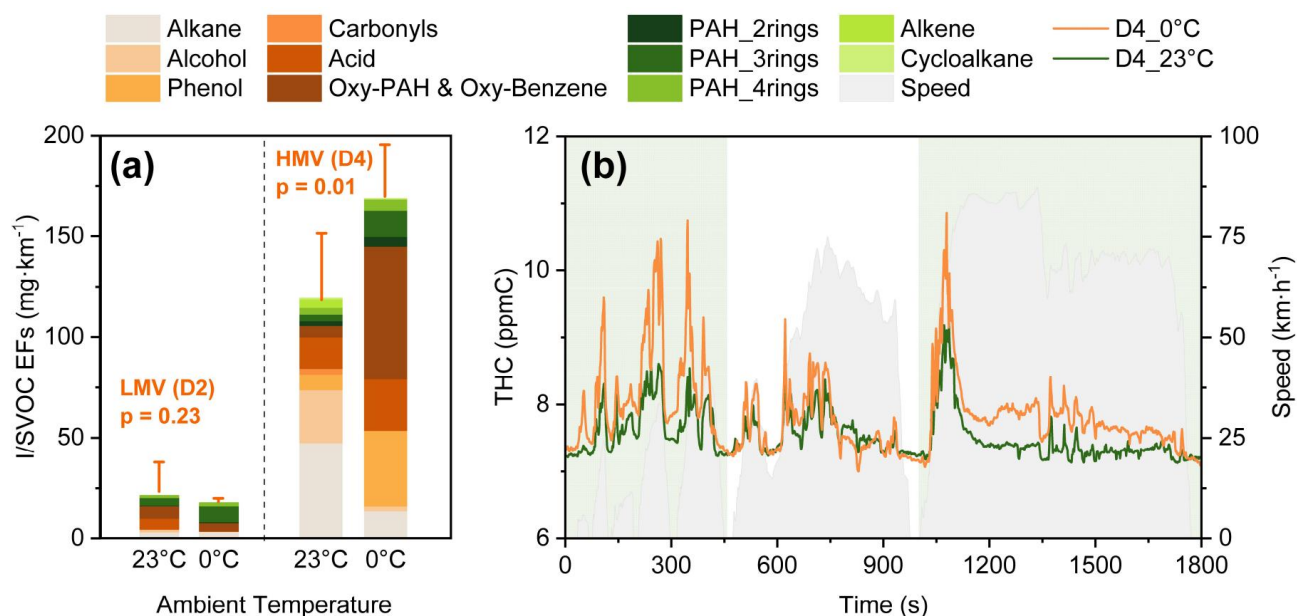
260 **Figure 2. The average volatility distribution of I/SVOCs of LMVs and HMVs.** The red dots represent the EF ratio of  
 HMV and LMV I/SVOCs (HMVs: LMVs). For the circular graph, different colored blocks represent the proportion of  
 different organic groups in I/SVOCs, where the inner ring represents average data from LMVs and the outer ring from  
 HMVs.



### 3.4 Low ambient temperature effect on total I/SVOC EFs and composition

The I/SVOC emissions during the hot-start cycle from LMV (D2) and H MV (D4) were tested at ambient temperatures of 0°C and 23°C. As shown in Figure 3(a), colder ambient temperature increased the total I/SVOC EF of H MV from 127 mg·km<sup>-1</sup> to 171 mg·km<sup>-1</sup> (p = 0.01). In contrast, no statistically significant increase was observed for the LMV (p = 0.23). Figure S7 shows the strong linear correlation (R<sup>2</sup> = 0.93) between I/SVOC EFs and MCE for LMVs and H MVs across different ambient temperatures. This finding suggests that the decline in MCE is a primary driver of the increase in I/SVOC EFs. Additionally, the MCE of LMVs exhibited greater stability, which explains the absence of elevated I/SVOC emissions at low ambient temperatures in comparison to H MVs. These results indicate that cumulative mileage enhances the sensitivity of I/SVOC emissions to ambient temperature. Even in the absence of instantaneous emission data of I/SVOCs at different ambient temperatures, the strong linear correlation between THC and I/SVOCs allows us to infer the instantaneous THC emission profile. Figure 3(b) illustrates that H MV was more likely to emit higher I/SVOC levels than LMV during rapid acceleration phases at 0°C, such as those occurring from 210 s to 220 s or from 1011 s to 1032 s. Furthermore, prior study has demonstrated that low temperatures significantly affect VOC emissions from diesel vehicles during cold-start conditions (Dardiotis et al., 2013). Therefore, we recommend that future studies focus on the I/SVOC emissions of vehicles during low-temperature cold-start conditions.

Regarding the distribution of I/SVOC categories, the mass fraction of PAHs increased at lower temperatures for both vehicle types (LMV: from 17% to 52%, H MV: from 10% to 14%). Given the toxicity of PAH, further research on the changes in exhaust gas toxicity in low-temperature environments is warranted, as the elevated PAH emissions may result from incomplete combustion under cold conditions. Additionally, the proportion of O-I/SVOCs in H MV increased from 52% to 78%, while no such trend was observed in LMV. Within the O-I/SVOCs of H MV, there was a notable decrease in alcohol, accompanied by a significant increase in carbonyls and oxy-PAH & oxy-benzene from 23°C to 0°C. This substantial increment of O-I/SVOC is expected to influence the SOA yield, as O-I/SVOCs typically exhibit lower SOAFP compared to hydrocarbon-like organics, such as alkanes (Chacon-Madrid and Donahue, 2011).



285 **Figure 3. (a) Total I/SVOC EFs of D2 and D4 at 0°C and 23°C. Different colored bars represent different organic groups. (b) The average instantaneous THC emission concentration of D4 at 0°C (orange line) and 23°C (green line).**

### 3.5 SOAFP of the I/SVOCs

To evaluate the environmental impact of HDDV exhaust, Figure 4 depicts the average potential SOA production after 48

hours of photooxidation. The estimated SOAFP of HMTVs reached  $30 \text{ mg}\cdot\text{km}^{-1}$ , approximately four times higher than that of  
290 LMVs ( $8 \text{ mg}\cdot\text{km}^{-1}$ ). However, the four-fold increase in SOAFP with cumulative mileage was less pronounced compared to the  
eight-fold increase observed for I/SVOC EFs. This discrepancy is primarily attributed to the greater increase in O-I/SVOC  
EFs relative to hydrocarbon-like organics (Chacon-Madrid and Donahue, 2011) (Sect. 3.3, Figure 2). The largest contributors  
to SOAFP for HMTVs were alkane (19%), oxy-PAH & oxy-benzene (18%), and phenol (18%), whereas, for LMVs, they were  
alkane (26%), acid (17%), and PAH\_3rings (17%). Therefore, alkane, oxy-PAH & oxy-benzene, and phenol were identified  
295 as the key contributors driving the increase in SOAFP for HMTVs.

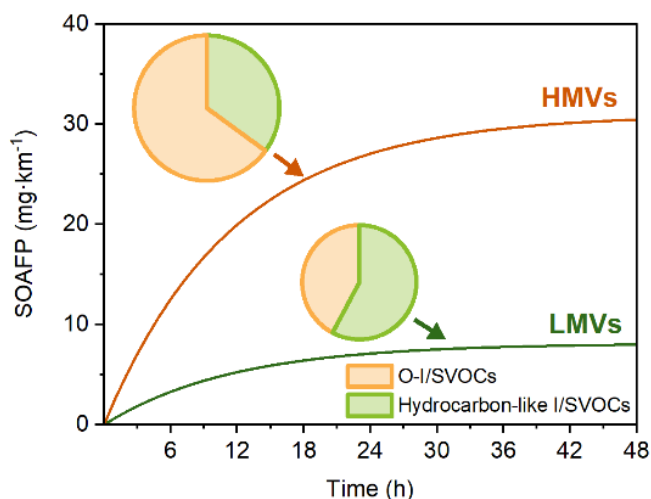


**Figure 4. The average SOAFP for HMTVs and LMVs during 48 h photooxidation.** The pie charts represent the contribution of hydrocarbon-like I/SVOCs and O-I/SVOCs to the total I/SVOC emissions of HMTVs and LMVs.

To estimate the effects of cumulative mileage and ambient temperature on the I/SVOC emission inventory, we constructed  
300 an emission inventory of China V HDDVs. In scenario 1, we utilized the average I/SVOC EFs of all tested vehicles, consistent  
with the approach taken in previous studies (Liu et al., 2021; Zhao et al., 2022; Wu et al., 2019; Zhang et al., 2024b). In  
scenario 2, the calculation was based on the assumption that the EFs increase linearly with cumulative mileage, as discussed  
in Sect. 3.3; Scenario 3 expanded on scenario 2 by incorporating an average ambient temperature of  $0^\circ\text{C}$  for three months of  
the year.

305 In 2022, the estimated I/SVOC emissions from China V HDDVs were 20, 60, and 66 kt for scenario 1, 2, and 3, respectively.  
The emissions in scenario 2 were up to three times higher than that in scenario 1. When considering the impact of low  
temperatures as in scenario 3, the total emissions increased by an additional 10%. Given the critical role of accurate HDDV  
I/SVOC emission inventories in predicting urban SOA formation, it is recommended that future studies measure and track  
I/SVOC emissions from HDDVs over extended periods (exceeding 3 years or corresponding to higher cumulative mileage).  
310 This will allow for a more comprehensive understanding of the degradation patterns of I/SVOCs from diesel vehicles.

#### 4 Conclusions

In this study, gaseous and particulate I/SVOCs emitted from four HDDVs were analyzed using TD-GC×GC-MS. The  
I/SVOC EFs from HDDVs ranged from 10 to  $409 \text{ mg}\cdot\text{km}^{-1}$ , with gaseous I/SVOCs contributing between 79% to 99% and  
315 particulate I/SVOCs accounting for 1% to 21%. The significant impact of vehicle cumulative mileage on I/SVOC emissions  
was evidenced by the eight times higher emissions from HMTVs compared with LMVs. The linear relationship between I/SVOC

emissions and vehicle cumulative mileage was established, emphasizing the need for long-term emission monitoring of HDDVs. Deterioration of I/SVOC emissions could occur under both cold-start and hot-running conditions, with comparable proportions of I/SVOC emissions during the cold-start cycles of HMs and LMs. Our findings suggest that emission deterioration factors should be incorporated into emission inventories for more accurate predictions of SOA formation. Furthermore, volatility and category distribution analysis revealed that the increase in I/SVOC emissions from HMV was primarily driven by higher-volatility compounds (bins 2 to 6).

Low ambient temperatures also increased I/SVOC emissions from HMs but not the case for LMs. A strong linear correlation ( $R^2 = 0.93$ ) between I/SVOC EFs and MCE from LMs and HMs across various temperatures suggests that the decline in combustion efficiency may be a direct cause of the increase. Changes in the composition of I/SVOCs at low temperatures were observed, with a notable increase in PAHs and oxygenated compounds, both of which are likely to influence SOA formation.

Finally, the SOAFP estimations revealed that the SOAFP of HMs was approximately four times higher than that of LMs after 48 hours of photooxidation. Furthermore, a China V I/SVOC emission inventory was established based on various assumptions. Results indicated that neglecting emission discrepancies between LMs and HMs could result in a threefold underestimation of inventory, while accounting for low temperatures would increase the total emissions by 10%. The study recommends incorporating the effects of cumulative mileage and temperature in future emission inventories for more accurate predictions of SOA formation.

### 335 **Associated content**

#### **Supporting information**

Additional experimental details, description of sampling sites, supplementary results, and supporting tables and figures.

#### **Author Contributions**

340 S.G.: Experiment, formal analysis, data validation, writing—original draft; X.Z.: Writing—reviewing and editing, project administration, supervision, funding acquisition; X.H.: Model development and funding acquisition; L.Z.: Experiment and funding acquisition; L.H. and X.W.: Experiment; Y. D.: Data validation; Z.H., T.C., and S.X.: Experiment; Y.Y.: Funding acquisition; S.X.: Editing; S.Z., J.J., and Y.W.: Data validation, writing—reviewing, and editing.

### 345 **Notes**

The authors declare no competing financial interest.

#### **Acknowledgments**

The authors acknowledge the financial support of the National Natural Science Foundation of China (grant nos. 51978404, 42261160645, 42105100, and 42307136), the Open Research Fund of Key Laboratory of Vehicle Emission Control and Simulation of Ministry of Ecology and Environment, Chinese Research Academy of Environmental Sciences (VECS2024K04), and the Fundamental Research Funds for the Central Public-interest Scientific Institution (2024YSKY-03), Macao Science and Technology Development Fund (0023/2022/AFJ and 001/2022/NIF), the Scientific Research Fund at Shenzhen University (grant nos. 868-000001032089 and 827-000907).

355

#### **References**

- Alam, M. S., Zeraati-Rezaei, S., Liang, Z., Stark, C., Xu, H., MacKenzie, A. R., and Harrison, R. M.: Mapping and quantifying isomer sets of hydrocarbons ( $\geq C_{12}$ ) in diesel exhaust, lubricating oil and diesel fuel samples using GC $\times$ GC-ToF-MS, *Atmos. Meas. Tech.*, 11, 3047–3058, <https://doi.org/10.5194/amt-11-3047-2018>, 2018.
- 360 Andrew F. May, Andrew A. May, Albert A. Presto, Christopher J. Hennigan, Ngoc T. Nguyen, T. D. Gordon, and Allen L. Robinson: Gas-particle partitioning of primary organic aerosol emissions: (2) diesel vehicles., *Environ. Sci. Technol.*, <https://doi.org/10.1021/es400782j>, 2013.
- Annual report on big data analysis of highway freight transport in China (2022), Chang'an University; China Transport Telecommunication & Information Center, China, 2022.
- 365 Aosaf, M. R., Wang, Y., and Du, K.: Comparison of the emission factors of air pollutants from gasoline, CNG, LPG and diesel fueled vehicles at idle speed, *Environmental Pollution*, 305, 119296, <https://doi.org/10.1016/j.envpol.2022.119296>, 2022.
- Apte, J. S., Brauer, M., Cohen, A. J., Ezzati, M., and Pope, C. A. I.: Ambient PM<sub>2.5</sub> reduces global and regional life expectancy, *Environ. Sci. Technol. Lett.*, 5, 546–551, <https://doi.org/10.1021/acs.estlett.8b00360>, 2018.
- 370 Azmi, S. and Sharma, M.: Global PM<sub>2.5</sub> and secondary organic aerosols (SOA) levels with sectorial contribution to anthropogenic and biogenic SOA formation, *Chemosphere*, 336, 139195, <https://doi.org/10.1016/j.chemosphere.2023.139195>, 2023.
- Cai, H. and Xie, S.: Temporal and spatial variation in recent vehicular emission inventories in China based on dynamic emission factors, *J. Air Waste. Manage.*, 63, 310–326, <https://doi.org/10.1080/10962247.2012.755138>, 2013.
- 375 Chacon-Madrid, H. J. and Donahue, N. M.: Fragmentation vs. functionalization: chemical aging and organic aerosol formation, *Atmos. Chem. Phys.*, 11, 10553–10563, <https://doi.org/10.5194/acp-11-10553-2011>, 2011.
- Chang, X., Zhao, B., Zheng, H., Wang, S., Cai, S., Guo, F., Gui, P., Huang, G., Wu, D., Han, L., Xing, J., Man, H., Hu, R., Liang, C., Xu, Q., Qiu, X., Ding, D., Liu, K., Han, R., Robinson, A. L., and Donahue, N. M.: Full-volatility emission framework corrects missing and underestimated secondary organic aerosol sources, *One Earth*, 5, 403–412, <https://doi.org/10.1016/j.oneear.2022.03.015>, 2022.
- 380 Cheng, Y., He, K. B., Duan, F. K., Zheng, M., Ma, Y. L., Tan, J. H., and Du, Z. Y.: Improved measurement of carbonaceous aerosol: evaluation of the sampling artifacts and inter-comparison of the thermal-optical analysis methods, *Atmospheric Chemistry and Physics*, 10, 8533–8548, <https://doi.org/10.5194/acp-10-8533-2010>, 2010.
- 385 Daniel S. Tkacik, Albert A. Presto, Neil M. Donahue, and Allen L. Robinson: Secondary organic aerosol formation from intermediate-volatility organic compounds: cyclic, linear, and branched alkanes, *Environ. Sci. Technol.*, <https://doi.org/10.1021/es301112c>, 2012.
- Dardiotis, C., Martini, G., Marotta, A., and Manfredi, U.: Low-temperature cold-start gaseous emissions of late technology passenger cars, *Applied Energy*, 111, 468–478, <https://doi.org/10.1016/j.apenergy.2013.04.093>, 2013.
- 390 Drozd, G. T., Weber, R. J., and Goldstein, A. H.: Highly resolved composition during diesel evaporation with modeled ozone and secondary aerosol formation: insights into pollutant formation from evaporative intermediate volatility organic compound sources, *Environ. Sci. Technol.*, 55, 5742–5751, <https://doi.org/10.1021/acs.est.0c08832>, 2021.
- Guan, T., Xue, T., Liu, Y., Zheng, Y., Fan, S., He, K., and Zhang, Q.: Differential susceptibility in ambient particle-related risk of first-ever stroke: findings from a national case-crossover study, *Am. J. Epidemiol.*, 187, 1001–1009,

395 <https://doi.org/10.1093/aje/kwy007>, 2018.

He, X., Wang, Q., Huang, X. H. H., Huang, D. D., Zhou, M., Qiao, L., Zhu, S., Ma, Y., Wang, H., Li, L., Huang, C., Xu, W., Worsnop, D. R., Goldstein, A. H., and Yu, J. Z.: Hourly measurements of organic molecular markers in urban Shanghai, China: Observation of enhanced formation of secondary organic aerosol during particulate matter episodic periods, *Atmos. Environ.*, 240, 117807, <https://doi.org/10.1016/j.atmosenv.2020.117807>, 2020.

400 He, X., Zheng, X., Zhang, S., Wang, X., Chen, T., Zhang, X., Huang, G., Cao, Y., He, L., Cao, X., Cheng, Y., Wang, S., and Wu, Y.: Comprehensive characterization of particulate intermediate-volatility and semi-volatile organic compounds (I/SVOCs) from heavy-duty diesel vehicles using two-dimensional gas chromatography time-of-flight mass spectrometry, *Atmos. Chem. Phys.*, 22, 13935–13947, <https://doi.org/10.5194/acp-22-13935-2022>, 2022a.

405 He, X., Zheng, X., You, Y., Zhang, S., Zhao, B., Wang, X., Huang, G., Chen, T., Cao, Y., He, L., Chang, X., Wang, S., and Wu, Y.: Comprehensive chemical characterization of gaseous I/SVOC emissions from heavy-duty diesel vehicles using two-dimensional gas chromatography time-of-flight mass spectrometry, *Environ. Pollut.*, 305, 119284, <https://doi.org/10.1016/j.envpol.2022.119284>, 2022b.

410 He, X., Zheng, X., Guo, S., Zeng, L., Chen, T., Yang, B., Xiao, S., Wang, Q., Li, Z., You, Y., Zhang, S., and Wu, Y.: Automated compound speciation, cluster analysis, and quantification of organic vapors and aerosols using comprehensive two-dimensional gas chromatography and mass spectrometry, *Atmos. Chem. Phys.*, 24, 10655–10666, <https://doi.org/10.5194/acp-24-10655-2024>, 2024.

Ho, K.: Thermodynamic formulation of a viscoplastic constitutive model capturing unusual loading rate sensitivity, *Int. J. Eng. Sci.*, 100, 162–170, <https://doi.org/10.1016/j.ijengsci.2015.12.003>, 2016.

415 Huang, C., Lou, D., Hu, Z., Feng, Q., Chen, Y., Chen, C., Tan, P., and Yao, D.: A PEMS study of the emissions of gaseous pollutants and ultrafine particles from gasoline- and diesel-fueled vehicles, *Atmos. Environ.*, 77, 703–710, <https://doi.org/10.1016/j.atmosenv.2013.05.059>, 2013.

420 Huang, D. D., Hu, Q., He, X., Huang, R.-J., Ding, X., Ma, Y., Feng, X., Jing, S., Li, Y., Lu, J., Gao, Y., Chang, Y., Shi, X., Qian, C., Yan, C., Lou, S., Wang, H., and Huang, C.: Obscured contribution of oxygenated intermediate-volatility organic compounds to secondary organic aerosol formation from gasoline vehicle emissions, *Environ. Sci. Technol.*, 58, 10652–10663, <https://doi.org/10.1021/acs.est.3c08536>, 2024.

Huang, L., Liu, H., Yarwood, G., Wilson, G., Tao, J., Han, Z., Ji, D., Wang, Y., and Li, L.: Modeling of secondary organic aerosols (SOA) based on two commonly used air quality models in China: Consistent S/IVOCs contribution but large differences in SOA aging, *Sci Total Environ*, 903, 166162, <https://doi.org/10.1016/j.scitotenv.2023.166162>, 2023.

425 Huang, R.-J., Zhang, Y., Bozzetti, C., Ho, K.-F., Cao, J.-J., Han, Y., Daellenbach, K. R., Slowik, J. G., Platt, S. M., Canonaco, F., Zotter, P., Wolf, R., Pieber, S. M., Bruns, E. A., Crippa, M., Ciarelli, G., Piazzalunga, A., Schwikowski, M., Abbaszade, G., Schnelle-Kreis, J., Zimmermann, R., An, Z., Szidat, S., Baltensperger, U., Haddad, I. E., and Prévôt, A. S. H.: High secondary aerosol contribution to particulate pollution during haze events in China, *Nature*, 514, 218–222, <https://doi.org/10.1038/nature13774>, 2014.

430 Jathar, S. H., Miracolo, M. A., Tkacik, D. S., Donahue, N. M., Adams, P. J., and Robinson, A. L.: Secondary organic aerosol formation from photo-oxidation of unburned fuel: experimental results and implications for aerosol formation from combustion emissions, *Environ. Sci. Technol.*, 47, 12886–12893, <https://doi.org/10.1021/es403445q>, 2013.

Kirchstetter, T. W., Corrigan, C. E., and Novakov, T.: Laboratory and field investigation of the adsorption of gaseous organic compounds onto quartz filters, *Atmos. Environ.*, 35, 1663–1671, [https://doi.org/10.1016/S1352-2310\(00\)00448-9](https://doi.org/10.1016/S1352-2310(00)00448-9), 2001.

- Li, X., Yang, Z., Fu, P., Yu, J., Lang, Y., Liu, D., Ono, K., and Kawamura, K.: High abundances of dicarboxylic acids, oxocarboxylic acids, and  $\alpha$ -dicarbonyls in fine aerosols (PM<sub>2.5</sub>) in Chengdu, China during wintertime haze pollution, *Environ. Sci. Pollut. Res.*, 22, 12902–12918, <https://doi.org/10.1007/s11356-015-4548-x>, 2015.
- Liu, Y., Li, Y., Yuan, Z., Wang, H., Sha, Q., Lou, S., Liu, Y., Hao, Y., Duan, L., Ye, P., Zheng, J., Yuan, B., and Shao, M.: Identification of two main origins of intermediate-volatility organic compound emissions from vehicles in China through two-phase simultaneous characterization, *Environ. Pollut.*, 281, 117020, <https://doi.org/10.1016/j.envpol.2021.117020>, 2021.
- Lu, Q., Zhao, Y., and Robinson, A. L.: Comprehensive organic emission profiles for gasoline, diesel, and gas-turbine engines including intermediate and semi-volatile organic compound emissions, *Atmos. Chem. Phys.*, 18, 17637–17654, <https://doi.org/10.5194/acp-18-17637-2018>, 2018.
- Lv, L., Ge, Y., Ji, Z., Tan, J., Wang, X., Hao, L., Wang, Z., Zhang, M., Wang, C., and Liu, H.: Regulated emission characteristics of in-use LNG and diesel semi-trailer towing vehicles under real driving conditions using PEMS, *J. Environ. Sci.*, 88, 155–164, <https://doi.org/10.1016/j.jes.2019.07.020>, 2020.
- Ministry of Ecology and Environment of the People's Republic of China: Technical guidelines for the preparation of integrated emission inventories of air pollutants and greenhouse gases, 2024.
- Morino, Y., Li, Y., Fujitani, Y., Sato, K., Inomata, S., Tanabe, K., Jathar, S. H., Kondo, Y., Nakayama, T., Fushimi, A., Takami, A., and Kobayashi, S.: Secondary organic aerosol formation from gasoline and diesel vehicle exhaust under light and dark conditions, *Environ. Sci.: Atmos.*, 2, 46–64, <https://doi.org/10.1039/D1EA00045D>, 2022.
- Presto, A. A., Miracolo, M. A., Kroll, J. H., Worsnop, D. R., Robinson, A. L., and Donahue, N. M.: Intermediate-volatility organic compounds: a potential source of ambient oxidized organic aerosol, *Environ. Sci. Technol.*, 43, 4744–4749, <https://doi.org/10.1021/es803219q>, 2009.
- Qi, L., Liu, H., Shen, X., Fu, M., Huang, F., Man, H., Deng, F., Shaikh, A. A., Wang, X., Dong, R., Song, C., and He, K.: Intermediate-volatility organic compound emissions from nonroad construction machinery under different operation modes, *Environ. Sci. Technol.*, 53, 13832–13840, <https://doi.org/10.1021/acs.est.9b01316>, 2019.
- Qi, L., Zhao, J., Li, Q., Su, S., Lai, Y., Deng, F., Man, H., Wang, X., Shen, X., Lin, Y., Ding, Y., and Liu, H.: Primary organic gas emissions from gasoline vehicles in China: Factors, composition and trends, *Environ. Pollut.*, 290, <https://doi.org/10.1016/j.envpol.2021.117984>, 2021.
- Sommers, J. M., Stroud, C. A., Adam, M. G., O'Brien, J., Brook, J. R., Hayden, K., Lee, A. K. Y., Li, K., Liggio, J., Mihele, C., Mittermeier, R. L., Stevens, R. G., Wolde, M., Zuend, A., and Hayes, P. L.: Evaluating SOA formation from different sources of semi- and intermediate-volatility organic compounds from the Athabasca oil sands, *Environ. Sci.: Atmos.*, 2, 469–490, <https://doi.org/10.1039/D1EA00053E>, 2022.
- Sun, P., Nie, W., Wang, T., Chi, X., Huang, X., Xu, Z., Zhu, C., Wang, L., Qi, X., Zhang, Q., and Ding, A.: Impact of air transport and secondary formation on haze pollution in the Yangtze River Delta: In situ online observations in Shanghai and Nanjing, *Atmos. Environ.*, 225, 117350, <https://doi.org/10.1016/j.atmosenv.2020.117350>, 2020.
- Tang, R., Lu, Q., Guo, S., Wang, H., Song, K., Yu, Y., Tan, R., Liu, K., Shen, R., Chen, S., Zeng, L., Jorga, S. D., Zhang, Z., Zhang, W., Shuai, S., and Robinson, A. L.: Measurement report: Distinct emissions and volatility distribution of intermediate-volatility organic compounds from on-road Chinese gasoline vehicles: implication of high secondary organic aerosol formation potential, *Atmos. Chem. Phys.*, 21, 2569–2583, <https://doi.org/10.5194/acp-21-2569-2021>, 2021.
- Tolouei, R. and Titheridge, H.: Vehicle mass as a determinant of fuel consumption and secondary safety performance,

- Transportation Research Part D: Transport and Environment, 14, 385–399, <https://doi.org/10.1016/j.trd.2009.01.005>, 2009.
- 475 Wang, Q., Huo, J., Chen, H., Duan, Y., Fu, Q., Sun, Y., Zhang, K., Huang, L., Wang, Y., Tan, J., Li, L., Wang, L., Li, D., George, C., Mellouki, A., and Chen, J.: Traffic, marine ships and nucleation as the main sources of ultrafine particles in suburban Shanghai, China, *Environ. Sci.: Atmos.*, 3, 1805–1819, <https://doi.org/10.1039/D3EA00096F>, 2023.
- 480 Wang, Y., Ning, M., Su, Q., Wang, L., Jiang, S., Feng, Y., Wu, W., Tang, Q., Hou, S., Bian, J., Huang, L., Lu, G., Manomaiphiboon, K., Kaynak, B., Zhang, K., Chen, H., and Li, L.: Designing regional joint prevention and control schemes of PM<sub>2.5</sub> based on source apportionment of chemical transport model: A case study of a heavy pollution episode, *Journal of Cleaner Production*, 455, 142313, <https://doi.org/10.1016/j.jclepro.2024.142313>, 2024.
- Wu, L., Wang, X., Lu, S., Shao, M., and Ling, Z.: Emission inventory of semi-volatile and intermediate-volatility organic compounds and their effects on secondary organic aerosol over the Pearl River Delta region, *Atmos. Chem. Phys.*, 19, 8141–8161, <https://doi.org/10.5194/acp-19-8141-2019>, 2019.
- 485 Xue, T., Han, Y., Fan, Y., Zheng, Y., Geng, G., Zhang, Q., and Zhu, T.: Association between a rapid reduction in air particle pollution and improved lung function in adults, *Annals ATS*, 18, 247–256, <https://doi.org/10.1513/AnnalsATS.202003-246OC>, 2021.
- Yao, Z., Wu, B., Wu, Y., Cao, X., and Jiang, X.: Comparison of NO<sub>x</sub> emissions from China III and China IV in-use diesel trucks based on on-road measurements, *Atmos. Environ.*, 123, 1–8, <https://doi.org/10.1016/j.atmosenv.2015.10.056>, 2015.
- 490 Zeng, L., Xiao, S., Dai, Y., Chen, T., Wang, H., Yang, P., Huang, G., Yan, M., You, Y., Zheng, X., Zhang, S., and Wu, Y.: Characterization of on-road nitrogen oxides and black carbon emissions from high emitters of heavy-duty diesel vehicles in China, *Journal of Hazardous Materials*, 477, 135225, <https://doi.org/10.1016/j.jhazmat.2024.135225>, 2024.
- Zhang, J., Wang, H., Yan, L., Ding, W., Liu, R., Wang, H., and Wang, S.: Analysis of chemical composition characteristics and source of PM<sub>2.5</sub> under different pollution degrees in autumn and winter of Liaocheng, China, *Atmosphere*, 12, 1180, <https://doi.org/10.3390/atmos12091180>, 2021.
- 495 Zhang, X., He, X., Cao, Y., Chen, T., Zheng, X., Zhang, S., and Wu, Y.: Comprehensive characterization of speciated volatile organic compounds (VOCs), gas-phase and particle-phase intermediate- and semi-volatile volatility organic compounds (I/S-VOCs) from Chinese diesel trucks, *Sci. Total Environ.*, 912, 168950, <https://doi.org/10.1016/j.scitotenv.2023.168950>, 2024a.
- 500 Zhang, Z., Man, H., Zhao, J., Huang, W., Huang, C., Jing, S., Luo, Z., Zhao, X., Chen, D., He, K., and Liu, H.: VOC and IVOC emission features and inventory of motorcycles in China, *J. Hazard. Mater.*, 469, 133928, <https://doi.org/10.1016/j.jhazmat.2024.133928>, 2024b.
- Zhao, J., Qi, L., Lv, Z., Wang, X., Deng, F., Zhang, Z., Luo, Z., Bie, P., He, K., and Liu, H.: An updated comprehensive IVOC emission inventory for mobile sources in China, *Sci. Total Environ.*, 851, 158312, <https://doi.org/10.1016/j.scitotenv.2022.158312>, 2022.
- 505 Zhao, Y., Hennigan, C. J., May, A. A., Tkacik, D. S., de Gouw, J. A., Gilman, J. B., Kuster, W. C., Borbon, A., and Robinson, A. L.: Intermediate-volatility organic compounds: a large source of secondary organic aerosol, *Environ. Sci. Technol.*, 48, 13743–13750, <https://doi.org/10.1021/es5035188>, 2014.
- Zhao, Y., Nguyen, N. T., Presto, A. A., Hennigan, C. J., May, A. A., and Robinson, A. L.: Intermediate volatility organic compound emissions from on-road diesel vehicles: chemical composition, emission factors, and estimated secondary organic aerosol production, *Environ. Sci. Technol.*, 49, 11516–11526, <https://doi.org/10.1021/acs.est.5b02841>, 2015.

510 Zhao, Y., Nguyen, N. T., Presto, A. A., Hennigan, C. J., May, A. A., and Robinson, A. L.: Intermediate volatility organic compound emissions from on-road gasoline vehicles and small off-road gasoline engines, *Environ. Sci. Technol.*, 50, 4554–4563, <https://doi.org/10.1021/acs.est.5b06247>, 2016.